Analysis of Lamb-Wave Dispersion and Band Gaps of Two-dimensional Piezoelectric Ponomic-Crystal Plates

Jin-Chen Hsu and Tsung-Tsong Wu

Institute of Applied Mechanics, National Taiwan University, Taipei 106, Taiwan

***Abstract*—Based on Mindlin's piezoelectric plate theory and the plane wave expansion (PWE) method, an eigen-matrix is formulated to study the frequency band gaps and dispersion relations of the lower-order Lamb waves in two-dimensional (2D) piezoelectric phononic plates. The phononic plates analyzed are composed of solid-solid and air-solid constituents with square and/or triangular lattices. Factors that influence the opening and width of the complete band gaps of Lamb waves are identified and discussed. For solid/solid phononic plates, the filling material chosen with a larger mass density, proper stiffness, and weak anisotropic factor embedded in a soft background material is suggested to obtain wider complete band gaps in the lower bands. On the other hand, for air/solid phononic plates, to achieve the complete band gaps are relatively difficult, and the background material itself with a proper anisotropy and a high filling fraction of air holes may favor the band-gap formation.**

I. Introduction

In recent years, there has been a growing interest in studying the properties of acoustic wave propagation in the composite materials, called phononic crystals (PCs), whose mass densities and elastic constants are periodically arranged in space [1]. The interest in these materials arises mainly from that they give rise to complete acoustic stop bands, which are analogous to the photonic band gaps for optical waves in photonic crystals [2] and may find promising applications to engineering such as acoustic wave guiding, filtering, and vibration shielding [3]-[4]. In addition to those phononic structures abundantly dealing with the bulk acoustic modes traveling in the interior of the medium and the surface acoustic modes on a truncated free surface of the structure [5]-[6], very recent studies show that another worthwhile category of phononic structures would be the periodic plates of finite thickness whereby the Lamb waves can propagate in [7]-[8]. On the other hand, it is worth noting that Lamb modes have been important in a variety of resonators, sensors, and characterization of elastic properties of thin films [9].

Among the existing studies, a lot of theoretical methods have been successfully applied to analyze the bulk acoustic waves in infinite phononic crystals; however, it is not always a straight forward task to adapt these methods for phononic plate problems. Based on the classical plate theory and three-dimensional equations of motion with suitable boundary conditions, respectively, the PWE method is used to address the phononic plate problems [7]. By using the on-shell layer-multiple-scattering theory, the guided and quasiguided elastic waves in a glass plate coated on one side with a period monolayer of polymer spheres, immersed in water, were studied [10]. Applying Bloch theorem of a periodic medium to the FEM formulation, the frequency band structures of Lamb waves in phononic plate consisting of quartz inclusions arranged periodically in an epoxy host were calculated and analyzed [8]. Recently, the Mindlin's plate theory based PWE method has been developed to serve as a concise and efficient way in analyzing the frequency band structures of lower-order Lamb modes in lower bands for non-piezoelectric phononic plates [7].

The purpose of this paper is to develop a PWE formulation for a piezoelectric phononic plate based on Mindlin's theory of piezoelectric crystal plate [11] and discuss the dispersion and band gaps of the Lamb modes. The analyzed structure is an infinite periodic plate with a finite thickness consisting of an array of cylindrical inclusions embedded in a hosting material, where the inclusions and/or the hosting material of the plate can be considered as piezoelectric solids here.

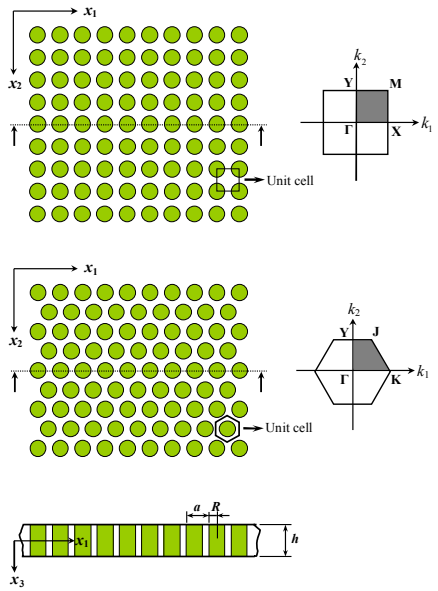

Figure 1. Top views and cross-section of infinite two-dimensional phononic-crystal plates with square and triangular lattices. Right-hand sketches are the corresponding first Brillouin zone.

II. Mindlin's Theory Based PWE Method

Consider a plate with thickness h whose material properties are homogeneous along the thickness. The coordinates are set up as follows. The x_3-axis be the thickness direction and directed downward, and the x_1-x_2 plane rests in the middle plane of the plate. Mindlin's two-dimensional theory gives [11]

$$\rho\frac{\partial^2 u_1^{(0)}}{\partial t^2}=\frac{\partial}{\partial x_1}\left[g_{11}u_{1,1}^{(0)}+g_{12}u_{2,2}^{(0)}+\kappa_2 g_{14}\left(u_{3,2}^{(0)}+u_2^{(1)}\right)+\breve{e}_{11}\phi_{,1}^{(0)}\right]$$
$$+\frac{\partial}{\partial x_2}\left[\kappa_1 c_{56}\left(u_{3,1}^{(0)}+u_1^{(1)}\right)+c_{66}\left(u_{2,1}^{(0)}+u_{1,2}^{(0)}\right)+e_{26}\phi_{,2}^{(0)}+e_{36}\phi^{(1)}\right],$$

$$\rho\frac{\partial^2 u_2^{(0)}}{\partial t^2}=\frac{\partial}{\partial x_1}\left[\kappa_1 c_{56}\left(u_{3,1}^{(0)}+u_1^{(1)}\right)+c_{66}\left(u_{2,1}^{(0)}+u_{1,2}^{(0)}\right)+e_{26}\phi_{,2}^{(0)}+e_{36}\phi^{(1)}\right]$$
$$+\frac{\partial}{\partial x_2}\left[g_{12}u_{1,1}^{(0)}+g_{22}u_{2,2}^{(0)}+\kappa_2 g_{24}\left(u_{3,2}^{(0)}+u_2^{(1)}\right)+\breve{e}_{12}\phi_{,1}^{(0)}\right],$$

$$\rho\frac{\partial^2 u_3^{(0)}}{\partial t^2}=\frac{\partial}{\partial x_1}\left[\kappa_1^2 c_{55}\left(u_{3,1}^{(0)}+u_1^{(1)}\right)+\kappa_1 c_{56}\left(u_{2,1}^{(0)}+u_{1,2}^{(0)}\right)+\kappa_1 e_{25}\phi_{,2}^{(0)}+\kappa_1\breve{e}_{35}\phi^{(1)}\right]$$
$$+\frac{\partial}{\partial x_2}\left[\kappa_2 g_{14}u_{1,1}^{(0)}+\kappa_2 g_{24}u_{2,2}^{(0)}+\kappa_2^2 g_{44}\left(u_{3,2}^{(0)}+u_2^{(1)}\right)+\kappa_2\breve{e}_{12}\phi_{,1}^{(0)}\right],$$

$$0=\frac{\partial}{\partial x_1}\left[\breve{e}_{11}u_{1,1}^{(0)}+\breve{e}_{22}u_{2,2}^{(0)}+\kappa_2\breve{e}_{14}\phi_{,2}^{(0)}-\varepsilon_{11}\phi_{,1}^{(0)}\right]$$
$$+\frac{\partial}{\partial x_2}\left[e_{26}\left(u_{1,2}^{(0)}+u_{2,1}^{(0)}\right)+\kappa_1 e_{25}\left(u_{3,1}^{(0)}+u_1^{(1)}\right)-\varepsilon_{22}\phi_{,2}^{(0)}-\varepsilon_{23}\phi^{(1)}\right],$$

$$\frac{\rho h^3}{12}\frac{\partial^2 u_1^{(1)}}{\partial t^2}=-h\left[\kappa_1^2 c_{55}\left(u_{3,1}^{(0)}+u_1^{(1)}\right)+\kappa_1 c_{66}\left(u_{2,1}^{(0)}+u_{1,2}^{(0)}\right)+\kappa_1 e_{25}\phi_{,2}^{(0)}+\kappa_1 e_{35}\phi^{(1)}\right]$$
$$+\frac{h^3}{12}\frac{\partial}{\partial x_1}\left[\gamma_{11}u_{1,1}^{(1)}+\gamma_{12}u_{2,2}^{(1)}+\hat{e}_{11}\phi_{,1}^{(1)}\right]+\frac{h^3}{12}\frac{\partial}{\partial x_2}\left[\gamma_{66}\left(u_{2,1}^{(1)}+u_{1,2}^{(1)}\right)+\hat{e}_{26}\phi_{,2}^{(1)}\right],$$

$$\frac{\rho h^3}{12}\frac{\partial^2 u_2^{(1)}}{\partial t^2}=-h\left[\kappa_2 g_{14}u_{1,1}^{(0)}+\kappa_2 g_{24}u_{2,2}^{(0)}+\kappa_2^2 g_{44}\left(u_{3,2}^{(0)}+u_2^{(1)}\right)+\kappa_2\hat{e}_{14}\phi_{,1}^{(0)}\right]$$
$$+\frac{h^3}{12}\frac{\partial}{\partial x_1}\left[\gamma_{66}\left(u_{2,1}^{(1)}+u_{1,2}^{(1)}\right)+\hat{e}_{26}\phi_{,2}^{(1)}\right]+\frac{h^3}{12}\frac{\partial}{\partial x_2}\left[\gamma_{12}u_{1,1}^{(1)}+\gamma_{22}u_{2,2}^{(1)}+\hat{e}_{12}\phi_{,1}^{(1)}\right],$$

$$0=-h\left[e_{36}\left(u_{1,2}^{(0)}+u_{2,1}^{(0)}\right)+e_{35}\left(u_{3,1}^{(0)}+u_1^{(1)}\right)-\varepsilon_{32}\phi_{,2}^{(0)}-\varepsilon_{33}\phi^{(1)}\right]$$
$$+\frac{h^3}{12}\frac{\partial}{\partial x_1}\left[\hat{e}_{11}u_{1,1}^{(1)}+\hat{e}_{12}u_{2,2}^{(1)}-\varepsilon_{11}\phi_{,1}^{(1)}\right]+\frac{h^3}{12}\frac{\partial}{\partial x_2}\left[\hat{e}_{26}\left(u_{2,1}^{(1)}+u_{1,2}^{(1)}\right)-\varepsilon_{22}\phi_{,2}^{(1)}\right]. \tag{1}$$

where $u_j^{(p)}$ and $\phi^{(p)}$, (p=0, 1), are the pth order displacements and potential field, respectively. ρ is the mass density, and κ_1 and κ_2 are correction factors. c_{IJ}, e_{iJ}, and ε_{ij} are the elastic stiffness, piezoelectric constant, and permittivity, respectively. Moreover, the modified material constants are given by

$$g_{IJ}=c_{IJ}-\frac{c_{I3}c_{3J}}{c_{33}},\qquad \breve{e}_{IJ}=e_{IJ}-\frac{e_{I3}c_{3J}}{c_{33}}, \tag{2}$$

$$\gamma_{IJ}=\frac{\text{cofactor}\,|s_{IJ}|}{|s_{IJ}|},\qquad \hat{e}_{\alpha J}=s_{IK}e_{\alpha I}\gamma_{JK}. \tag{3}$$

The constant s_{IJ}, is elastic compliance, and the determinant is

$$|s_{IJ}|=\begin{vmatrix}s_{11}&s_{12}&2s_{16}\\ s_{21}&s_{22}&2s_{26}\\ 2s_{16}&2s_{26}&4s_{66}\end{vmatrix}. \tag{4}$$

Consider an infinite 2D piezoelectric phononic plate as shown in Fig. 1. In a periodic structure, the displacements and potential field satisfy the Bloch theorem. Therefore, in 2D case, the displacements and potential can be expressed as

(a)
$$\begin{aligned}u_j^{(0)}&=\sum_{\mathbf{G}}A_{\mathbf{G}}^{j}e^{i(\mathbf{G}+\mathbf{k})\cdot\mathbf{r}-i\omega t},\quad i=1,2,3,\\ \phi^{(0)}&=\sum_{\mathbf{G}}A_{\mathbf{G}}^{4}e^{i(\mathbf{G}+\mathbf{k})\cdot\mathbf{r}-i\omega t},\\ u_\alpha^{(1)}&=\sum_{\mathbf{G}}B_{\mathbf{G}}^{\alpha}e^{i(\mathbf{G}+\mathbf{k})\cdot\mathbf{r}-i\omega t},\quad \alpha=1,2,\\ \phi^{(1)}&=\sum_{\mathbf{G}}B_{\mathbf{G}}^{3}e^{i(\mathbf{G}+\mathbf{k})\cdot\mathbf{r}-i\omega t},\end{aligned} \tag{5}$$

where $\mathbf{r}=(x_1, x_2)$ is the 2D position vector, ω is the angular frequency, $\mathbf{k}=(k_1, k_2)$ is the Bloch wave vector in the two-dimensional Brillouin zone (BZ), and $\mathbf{G}=(G_1, G_2)$ is the two-dimensional reciprocal lattice vector. $A_{\mathbf{G}}^{j}$, $A_{\mathbf{G}}^{4}$, $B_{\mathbf{G}}^{\alpha}$, and $B_{\mathbf{G}}^{3}$ are the corresponding Fourier coefficients. The periodicity of the structure implies that the material properties $f(\mathbf{r})$ may all be expanded in the Fourier series:

(b)
$$f(\mathbf{r})=\sum_{\mathbf{G}}f_{\mathbf{G}}e^{i\mathbf{G}\cdot\mathbf{r}}, \tag{6}$$

Substituting Eq. (5) and Eq. (6) into Eq. (1), one can obtain a linear system of equations in the matrix form:

$$\begin{pmatrix}\mathbf{L}_{\mathbf{G},\mathbf{G}'}^{11}&\cdots&\mathbf{L}_{\mathbf{G},\mathbf{G}'}^{17}\\ \vdots&\ddots&\vdots\\ \mathbf{L}_{\mathbf{G},\mathbf{G}'}^{71}&\cdots&\mathbf{L}_{\mathbf{G},\mathbf{G}'}^{77}\end{pmatrix}\cdot\begin{pmatrix}\mathbf{A}_{\mathbf{G},\mathbf{G}'}^{1}\\ \mathbf{A}_{\mathbf{G},\mathbf{G}'}^{2}\\ \mathbf{A}_{\mathbf{G},\mathbf{G}'}^{3}\\ \mathbf{A}_{\mathbf{G},\mathbf{G}'}^{4}\\ \mathbf{B}_{\mathbf{G},\mathbf{G}'}^{1}\\ \mathbf{B}_{\mathbf{G},\mathbf{G}'}^{2}\\ \mathbf{B}_{\mathbf{G},\mathbf{G}'}^{3}\end{pmatrix}\equiv\mathbf{L}\cdot\begin{pmatrix}\mathbf{A}_{\mathbf{G},\mathbf{G}'}^{1}\\ \mathbf{A}_{\mathbf{G},\mathbf{G}'}^{2}\\ \mathbf{A}_{\mathbf{G},\mathbf{G}'}^{3}\\ \mathbf{A}_{\mathbf{G},\mathbf{G}'}^{4}\\ \mathbf{B}_{\mathbf{G},\mathbf{G}'}^{1}\\ \mathbf{B}_{\mathbf{G},\mathbf{G}'}^{2}\\ \mathbf{B}_{\mathbf{G},\mathbf{G}'}^{3}\end{pmatrix}=\mathbf{0}. \tag{7}$$

While the summation of Eqs. (5) and (6) are truncated up to n reciprocal lattice vectors $\mathbf{G}$ in practice, Matrix $\mathbf{L}$ in Eq. (13) is reduced to a 7n by 7n matrix. Each submatrix in $\mathbf{L}$ is a function of frequency, Bloch wave vector, reciprocal lattice vector, and Fourier coefficients. Eventually, the eigenfrequencies of Lamb waves are chosen by setting the condition: Det ($\mathbf{L}$)=0.

III. Numerical Calculations of Band Structures

The solid/solid piezoelectric phononic plates are illustrated with the Quartz/Epoxy and TeO_2/Epoxy combinations. First of all, Figs. 2(a) and (b) show the frequency band structures of Lamb waves propagating in the Quartz/Epoxy phononic plate

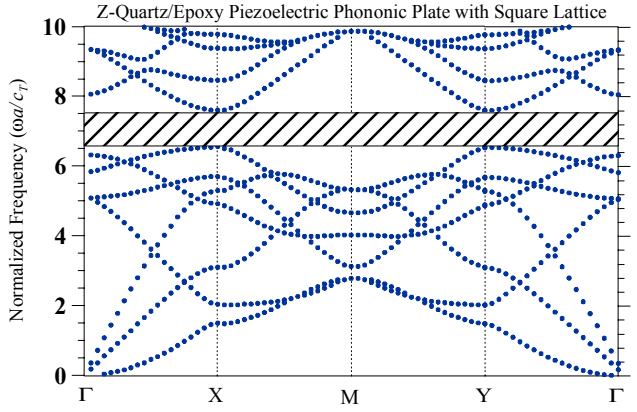

Figure 2. Band structure of Lamb waves in the 2D Quartz/Epoxy piezoelectric phononic plate with square lattice. The radius R of quartz inclusions and plate thickness h are 0.4a and 0.275a, respectively.

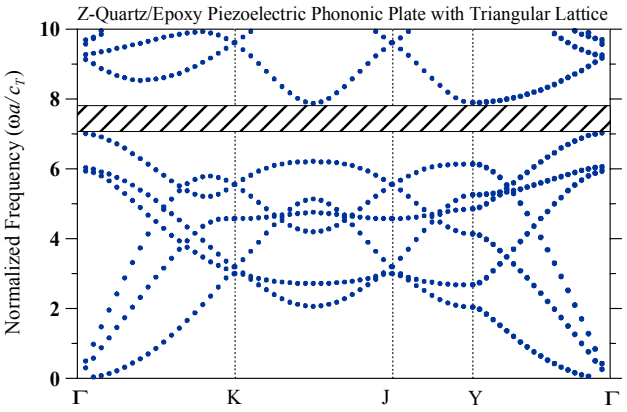

Figure 2. Band structure of Lamb waves in the 2D Quartz/Epoxy piezoelectric phononic plate with triangular lattice. The radius R of quartz inclusions and plate thickness h are 0.4a and 0.275a, respectively.

with SL and TL, respectively. The radius R of the quartz cylinders is set at 0.4a, and the plate thickness h=0.275a for both of the lattices. These calculated results are obtained by using 289 reciprocal lattice vectors such that a satisfactory convergence can be attained in the displayed frequency interval. The calculations are along the irreducible parts of the first Brillouin-zone (BZ) boundaries, as those depicted in Fig. 1. Shown in Fig. 2(a), the SL Quartz/Epoxy plate has a complete band gap of Lamb waves extended from 6.56 to 7.6 in the normalized unit; the band-gap width in terms of the ratio of the band gap width to its midgap frequency, therefore, is 14.7%. For that of the TL quartz/epoxy plate in Fig. 2(b), the lowest complete band gap ranges from 7.02 to 7.88, and the band-gap width is 11.5%. The Lamb-wave band gaps is slightly larger in the SL than in the TL for R=0.4a and h=0.275a.

Figures 3 and 4 display the band-gap distributions of the Quartz/Epoxy phononic plates simultaneously for the bulk waves and Lamb waves as a function of the filling fraction F (volume fraction of the inclusions in the structure). Figures 3 and 4 respectively refer to the SL and TL structures, and the plate thickness is h=0.275a. In Fig. 3, the distribution of the complete Lamb-wave gap is close to the two frequency regions of the complete bulk-wave gaps with a slightly down shift in frequency and overlapping with the first complete band gap of the bulk waves. The maximum band gap of Lamb waves for the SL Quartz/Epoxy plate takes place around F=0.45-0.5. For the TL structure in Fig. 4, a similar result is found, but there exists only one and larger complete band-gap region of bulk waves. The maximum complete Lamb-wave band gap for the TL Quartz/Epoxy phononic plate is at F=0.58. Note that the overlapping gaps of both bulk waves and Lamb waves can be regarded as the forbidden frequencies whenever the effects of the plate surfaces come into play or not as the waves propagate.

As another illustration, shown in Figs. 5 is the Lamb-wave band structure of the TeO_2/Epoxy plate. The plate thickness is remained at h=0.275a, and the radius of the TeO_2 inclusions is R=0.389a. Though the acoustic mismatches between TeO_2 and Epoxy are larger than that between Quartz and Epoxy; however, it can be observed that both of the lattices for this combination open just narrow complete band gaps. For the SL TeO_2/epoxy phononic plate, the complete band gap shown in Fig. 5 extends from 6.72 to 7.08 (5.2% in width). Additional

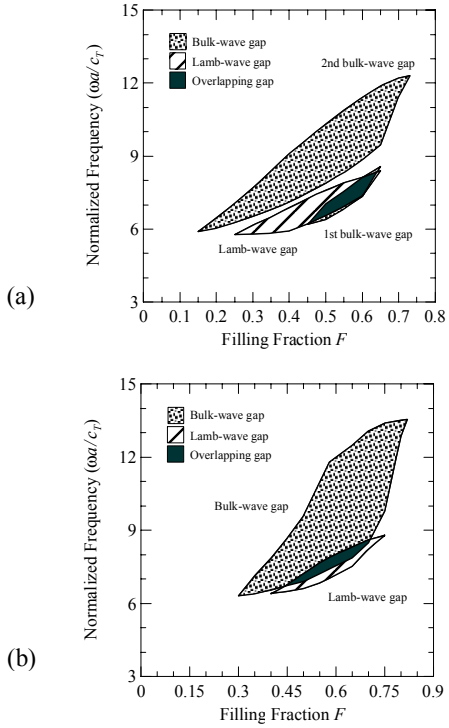

Figure 4. Band-gap distribution as a function of the filling feaction F for the TL Quartz/Epoxy piezoelectric plate. (a) For SL (b) For TL.

calculation for the TL TeO_2/epoxy plate shows that the gap is from 6.86 to 7.22 (5.1% in width). Even if change the radius R, the frequency band structures display no more than the narrow Lamb-wave band gaps. On the other hand, the variation of the plate thickness also will not effectively benefit to a wider Lamb-wave gap. A wider band gap expected to exist in the phononic structure with a acoustic mismatch as large as possible or inclusions as massive as possible is almost a rule of thumb, which drawn form the investigations of bulk acoustic waves in infinite phononic crystals composed of isotropic constituents; however, by present analyses, the same dose not hold for those of Lamb waves in the phononic plates consisting

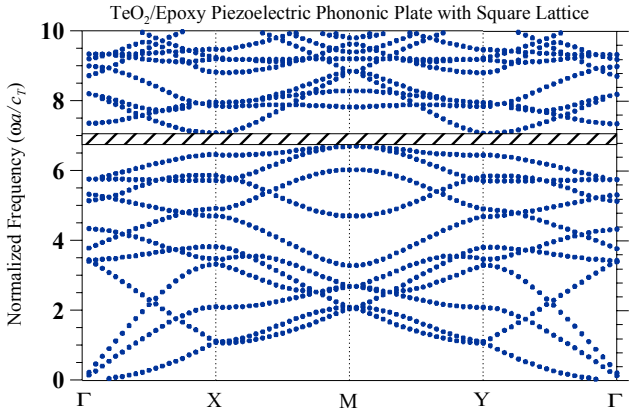

Figure 5. Band structure of Lamb waves in the 2D Quartz/Epoxy piezoelectric phononic-crystal plate with square lattice. The radius R of quartz inclusions and plate thickness h are 0.389a and 0.275a, respectively.

of anisotropic, piezoelectric components. In the case of TeO_2-epoxy structure, it can be explained by couple of reasons:

1. Smaller values of the elastic stiffness and larger density of the inclusions result in the lower phase velocities, and thus, dense the distributions of the frequency bands. For a thin plate, the flexural-dominated bands aggravate this.
2. The strong anisotropic factor (A=26.4) blocks the band gaps to be omnidirectional or reduces in the frequency width of the complete band gap.

For an air/solid plate, Fig. 6 shows the frequency band structure of Lamb waves in the SL Air/Quartz piezoelectric phononic plate. The radius of the circular air holes is R=0.44a (F=0.608), and the plate thickness is h=0.625a. This Lamb-wave band structure exhibits just a tiny complete band gap from 2.96 to 3.05 (3% in width). Although the air inclusions are very efficient reflectors for elastic waves with any polarization, the resulted complete band gap is much narrower than those created by the Quartz/Epoxy plates. The main reason is that the air inclusions can not be resonated to widen the band gap; therefore, only a smaller Bragg gap for Lamb modes can exist with these periodic air holes based on the Bragg scattering mechanism. And a high volume filling fraction is needed to intensify the direction-dependent scattering so that the gap can

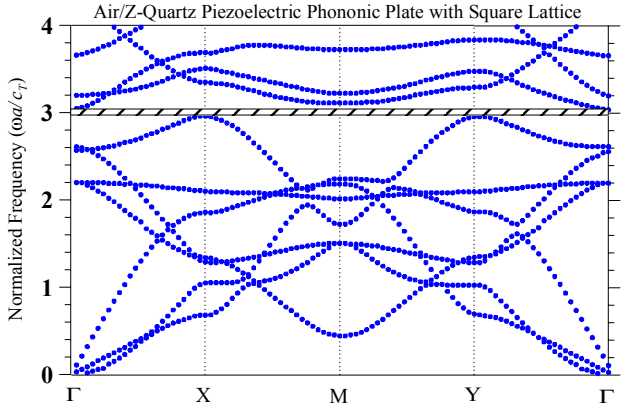

Figure 6. Band structure of Lamb waves in the 2D Air/Quartz piezoelectric phononic-crystal plate with square lattice. The radius R of quartz inclusions and plate thickness h are 0.44a and 0.625a, respectively.

open up as a complete gap. This complete Lamb-wave gaps of Air/Quartz plates are also highly sensitive to the plate thickness; the gap can sustain only a small variation of the plate thickness around h=0.625a. Finally, it is worth noting that the anisotropy of the background material itself of an air/solid phononic thin plate may not always be adverse to a complete band gap, yet can be a favorable factor to weaken the geometric anisotropy caused by the periodicity of the structure such that a complete band gap can open up.

IV. Conclusion

By utilizing Mindlin's plate theory based PWE method, the complete band gaps and dispersion relations of the lower-order Lamb waves propagating in 2D solid/solid and air/solid piezoelectric phononic plates have been analyzed. The eigen-matrix to calculate the dispersion relations has been derived. Some of the factors influence the opening and width of the complete Lamb-wave gaps are identified and discussed. For solid/solid phononic plates, the inclusions chosen with larger mass density, proper stiffness, and weak anisotropic factor embedded in a soft host is suggested to obtain wider complete band gaps for lower-order Lamb waves. For the Air/Quartz phononic plate, a narrower Lamb-wave gap is obtained with lacking the resonance mechanism. A background material itself with proper anisotropy may favor the opening of the complete band gaps for the air/solid plate.

Acknowledgment

The authors gratefully acknowledge the financial support of this research from the National Science Council of Taiwan.

References

[1] http://www.phys.uoa.gr/phononics/PhononicDatabase.html

[2] A. Modinos, N. Stefanou, I. E. Psarobas, and V. Yannopapas, "On wave propagation in inhomoheneous systems," *Physica B*, vol. 296, pp. 167-173, 2001

[3] Y. Pennec, B. Djafari-Rouhani, J. O. Vasseur, A. Khelif, and P. A. Deymier, "Tunable filtering and demultiplexing in phononic crystal with hollow cylinders," *Phys. Rev. B*, vol. 69, pp. 046608: 1-6, 2004.

[4] G. Wang, X. Wen, J. Wen, L. Shao, and Y. Liu, "Two-dimensional locally resonant phononic crystals with binary structures," *Phys. Rev. Lett.*, vol. 93, pp. 154302: 1-4, 2004.

[5] J.-C. Hsu and T.-T. Wu, "Bleustein-Gulyaev-Shimizu surface acoustic waves in two-dimensional piezoelectric phononic crystals," *IEEE Trans. Ultrason., Ferroelect., Freq. Contr.* vol. 53, pp. 1169-1176, 2006.

[6] T.-T. Wu, J.-C. Hsu, and Z.-G Huang, "Band gaps and the electromechanical coupling coefficient of a surface acoustic wave in a two-dimensional piezoelectric phononic crystals," *Phys. Rev. B*, vol. 71, pp. 064303: 1-5, 2005.

[7] J.-C. Hsu and T.-T. Wu, "Efficient formulation for band-structure calculations of two-dimensional phononic-crystal plates," *Phys. Rev. B*, vol. 74, pp. 144303: 1-7, 2006.

[8] A. Khelif, B. Aoubiza, S. Mohammadi, A. Adibi, and V. Laude, "Complete band gaps in two-dimensional phononic crystal slabs," *Phys. Rev. E*, vol. 74, pp. 046610: 1-5, 2006.

[9] S. W. Wenzel and R. M. White, "A multisensor employing an ultrasonic Lamb-wave oscillator," *IEEE Trans. Electron Devices*, vol. 35, pp. 735-743, 1988.

[10] R. Sainidou and N. Stefanou, "Guided and quasiguided waves in phononic crystal slabs," *Phys. Rev. B*, vol. 73, pp. 184301: 1-7, 2006.

[11] R. D. Mindlin, "High frequency vibrations of piezoelectric crystal plates," *Int. J. Solid Struct.*, vol. 8, pp. 895-906, 1972.